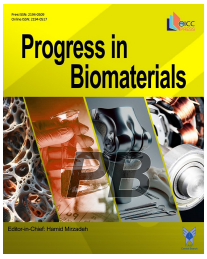

Volume 12, Issue 3, 122315 (1-14)

Progress in Biomaterials (PIBM)

https://doi.org/10.57647/pibm.2023.122315

Synthesis, *in Silico* Pharmaceutical Properties, Anticancer and Anti-Inflammatory Activities of Novel Benzo[b]thiophene Derivative

Shayesteh Poorhosein Ghazi Mahaleh[1,*], Muheb. A. S. Algso[2], Omruye Ozok Arici[3], Arif Kivrak[4], Sevki Arslan[1]

[1]*Department of Biology, Faculty of Science, Pamukkale University, Denizli 20160, Turkey.*
[2]*Department of Chemistry, College of Science, University of Duhok, Duhok 42001, Iraq.*
[3]*Biomedical Engineering, Faculty of Engineering and Architectural Science, Eskisehir Osmangazi University, Eskisehir 26040, Turkey.*
[4]*Department of Chemistry, Faculty of Science, Eskisehir Osmangazi University, Eskisehir 26040, Turkey.*

[*]**Corresponding author:** smahaleh18@posta.pau.edu.tr

Original Research

Received:
21 August 2023
Revised:
23 September 2023
Accepted:
28 September 2023
Published online:
30 September 2023

Abstract:

Sulfur-containing compounds have various biological functions, the most important of which are anti-inflammatory and anticancer effects. This study provides the first evaluation of the biological potential of a novel benzothiophene derivative, 3-iodo-2-phenylbenzo[b]thiophene (IPBT), with a special focus on its cytotoxic, anticancer, cell migration, colony formation and anti-inflammatory properties. The EC50 values of IPBT were determined in MDA-MB-231, HepG2, LNCaP, Caco-2, Panc-1, HeLa and Ishikawa cancer cell lines (126.67, 67.04, 127.59, 63.74, 76.72, 146.75 and 110.84 respectively). The compound was found to induce apoptosis by activating the expression levels of pro-apoptotic genes, *BAX*, *CASP3*, *CASP8*, *CASP9*, and *P53* in cancer cells and effectively inhibit cell migration and colony formation. IPBT, also significantly reduced inflammatory responses (Nitric oxide production) in LPS-induced RAW264.7 macrophage cells by proinflammatory genes (*COX-2*, *iNOS*, *TNF-α*, and *IL-6*). These findings suggest that IPBT may be a promising candidate for cancer treatment as well as a therapeutic agent for controlling inflammation and tissue repair.

Keywords: *In silico* synthesis; Anticancer activity; Anti-inflammatory; Benzo[b]thiophene

Cite this article: Ghazi Mahaleh, S. P., Algso, M. A. S., Ozok Arici, O., Kivrak, A., Arslan, S. Synthesis, in Silico Pharmaceutical Properties, Anticancer and Anti-Inflammatory Activities of Novel Benzo[b]thiophene Derivative. *Progress in Biomaterials* **12**(3), Article 15 (2023).

Introduction

Cancer remains one of the most concerning diseases and major global public health challenges, with increasing incidence and mortality rates worldwide (Hiremath et al., 2019; Ma & Yu, 2007). In 2020, an estimated 19.3 million new cases of cancer and almost 10 million deaths were reported globally (Sung et al., 2021), making cancer the second leading cause of death after cardiovascular disease in many countries (Ma & Yu, 2007). These figures place cancer as one of the leading causes of death worldwide (Cao et al., 2015). At the cellular level, cancer results from the failure of innate regulatory mechanisms that control cell proliferation and homeostasis (Haberkorn, 2007). Instead of responding appropriately to signals that regulate normal cell behavior, cancer cells proliferate uncontrollably, leading to the accumulation of abnormalities in various cellular regulatory systems that ultimately lead to cancer (Hanahan & Weinberg, 2011).

This dysregulation is usually caused by genetic mutations, aberrant activation of oncogenes, or disruption of homeostatic signaling pathways. From a biological perspective, these events enable cells to proliferate uncontrollably in

inappropriate spatial and temporal contexts, activate oncogenic pathways, inhibit appropriate differentiation, and invade surrounding tissues, ultimately leading to metastasis (Hegde & Chen, 2020; Pedraza-Fariña, 2007). Furthermore, tumor progression is not simply the result of intrinsic cellular abnormalities but is shaped by tumor–immune interactions. Some malignancies arise in chronically inflamed tissues, while others may hijack immune mechanisms to enhance their survival, growth, and metastatic potential (Zhao et al., 2021). Cancer treatment is a complex and ever-evolving medical challenge. While traditional methods such as surgery, chemotherapy, and radiotherapy are still commonly used, new techniques such as stem cell therapies, targeted therapies, nanotechnology-based interventions, natural antioxidants, and strategies guided by ferroptosis have emerged (Debela et al., 2021; Nie et al., 2022). However, despite these advances, many challenges remain, highlighting the need for research to increase the effectiveness of treatment and enhance patient outcomes (Pucci et al., 2019). Heterocyclic compounds play a significant role in modern organic chemistry, especially in drug discovery and optimization (Kalaria et al., 2018; Qadir et al., 2022). Among these compounds, benzothiophene and thiophenes are notable as excellent molecular scaffolds for the development of new drugs (Fakhr et al., 2009; Mishra et al., 2020; Rosada et al., 2019; Singh et al., 2020). Their planar structure, together with a sulfur atom with high electron density, enhances their interaction with enzymes and biological receptors. In addition, their polar characteristics improve key pharmacokinetic properties such as absorption, distribution and bioavailability (Kalaria et al., 2018). Furthermore, thiophene derivatives have attracted much attention due to their diverse biological activities (Singh et al., 2020), including antioxidant (Shah & Verma, 2019), anti-inflammatory (Haridevamuthu et al., 2022), antimicrobial (Mabkhot et al., 2019), and anticancer properties (Archna et al., 2020; Gad et al., 2020).

Their structural flexibility enables the synthesis of diverse derivatives with desirable pharmacological profiles, further enhancing their importance as valuable drug scaffolds. In this investigation, the anticancer and anti-inflammatory activities of a novel derivative, 3-iodo-2-phenylbenzo[b]thiophene (IPBT), were investigated. This compound was selected based on its promising structural features and remarkable biological efficacy in various therapeutic areas. To provide a more comprehensive assessment of its biological effects, PCR analysis, apoptosis assay, colony formation assays, and cell migration assays were performed. This study's findings offer fresh perspectives on the potential of benzothiophene derivatives as targeted therapeutic agents, particularly in cancer treatment.

Results

Synthesis of 3-iodo-2-phenylbenzo[b]thiophene (IPBT)

A palladium-catalyzed Sonogashira cross-coupling reaction, well recognized for its efficiency in forming carbon–carbon bonds between terminal alkynes and halogenated aromatic substrates, was employed for the synthesis of the target compound IPBT derivative. Triethylamine (Et3N) served as the base within a catalytic system comprising palladium and copper catalysts. Specifically, 2-iodo thioanisole (1) and ethynylbenzene (2) were reacted in the presence of $PdCl_2(PPh_3)_2$ and copper iodide (CuI) using triethylamine as the reaction medium. After obtaining the intermediate methyl(2-(phenylethynyl) phenyl) sulfane (3) (224 mg, 1 mmol), it was dissolved in dichloromethane (CH_2Cl_2, 5 mL), and iodine (I_2, 761 mg, 3 mmol) was added. The reaction was maintained under stirring at room temperature for 120 minutes. The reaction was then quenched with a saturated sodium thiosulfate ($Na_2S_2O_3$) solution and extracted with ethyl acetate (EtOAc). The combined organic layers were dried over anhydrous magnesium sulfate ($MgSO_4$), filtered, and the solvent was removed under reduced pressure. The crude residue underwent purification through column chromatography, resulting in the isolation of the desired IPBT compound as a white solid with a 98% yield (Fig. 1).

In silico assessment of IPBT drug properties

The pharmacokinetic potential and drug similarity of the benzothiophene-derived IPBT were assessed using Swiss computational ADME (absorption, distribution, metabolism, and excretion) analysis (Deng et al., 2022). The results of these analyses are presented in Fig. 2, while Table 1 provides detailed numerical data. Computational predictions indicate that IPBT can cross both the gastrointestinal and blood-brain barriers, as well as interact with and penetrate the P-glycoprotein (P-gp) efflux system.

Cytotoxicity evaluation of IPBT derivative using the MTT assay

The cytotoxic potential of the IPBT derivative was evaluated in MDA-MB-231, HepG2, LNCaP, Caco-2, Panc-1, HeLa, Ishikawa, and HUVEC cell lines following a 24-hour exposure at concentrations ranging from 0 to 250 μM, using the MTT assay (Table 2). The IPBT derivative exhibited a dose-dependent inhibition of cell viability and demonstrated significant cytotoxic effects across various cancer cell lines (Fig. 3). EC50 values were calculated for each cancer cell

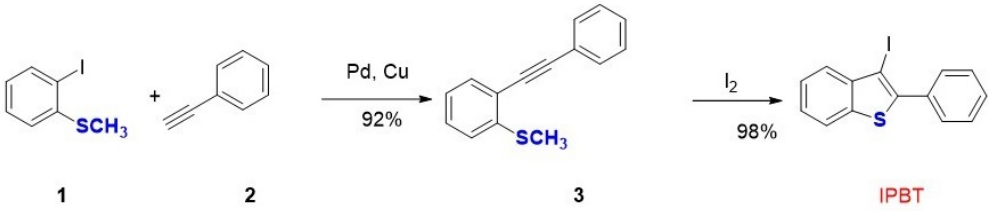

Figure 1. Synthesis of IPBT.

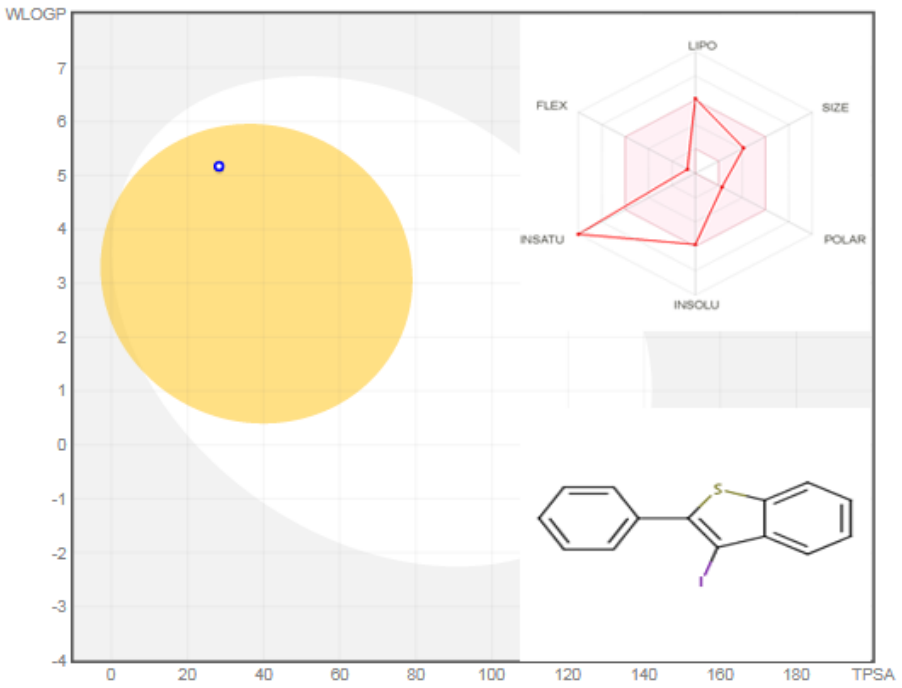

Figure 2. Calculated ADME properties of 3-iodo-2-phenylbenzo[b]thiophene (IPBT) in the BOILED-Egg diagram and radar plot.

line to quantify its potency (Table 2). Importantly, the viability of non-cancerous HUVEC cells remained above 50% after 24 hours of treatment (Fig. 3).

After 24-hour treatment of the cells with the IPBT compound, cytotoxicity was assessed via cell viability assays, and the data were statistically analyzed to determine the half-maximal effective concentration (EC50) values (Table 2).

Inhibition of clonogenic potential

Colony formation assays were performed on MDA-MB-231, HepG2, LNCaP, Caco-2, Panc-1, HeLa, and Ishikawa cell lines to evaluate the long-term effect (14 days) of IPBT on cancer cell growth. After treatment with IPBT at the

Table 1. Physicochemical and pharmacokinetic properties of IPBT.

Molecular formula	C14H9IS
Molecular weight	338.19 g/mol
Log Po/w (XLOGP3)	5.25
Log S (ESOL)	−5.88 (moderately soluble)
Log S (Ali)	−5.59 (moderately soluble)
Log S (SILICOS-IT)	−6.78 (poorly soluble)
GI absorption	High
BBB permeant	Yes
P-gp substrate	Yes
CYP1A2 inhibitor	Yes
CYP2C19 inhibitor	Yes
CYP2C9 inhibitor	Yes
CYP2D6 inhibitor	No
CYP3A4 inhibitor	No
Bioavailability score	0.55
PAINS	0 alert
Brenk	1 alert (iodine)
Leadlikeness	1 violation (XLOGP3 > 3.5)
Synthetic accessibility	2.58

Table 2. 24-hour EC50 (μM) values of IPBT derivative.

Cell	MDA-MB-231	HepG2	LNCaP	Caco-2	Panc-1	HeLa	Ishikawa	HUVEC
EC50(μM)	126.67	67.04	127.59	63.74	76.72	146.75	110.84	-

- EC50 $>$ 250 μM or inactive.

respective EC50 concentrations, the cells' ability to form colonies was assessed.

When colony numbers in the control groups were accepted as 100%, the colonies formed in IPBT-treated MDA-MB-231, HepG2, LNCaP, Caco-2, Panc-1, HeLa, and Ishikawa cells were 43.91%, 10.83%, 7.29%, 47.29%, 40.30%, 58.65%, and 88.82%, respectively (Fig. 4.1, 4.2 and Table 3).

IPBT treatment resulted in a significant reduction in colony formation across all tested cell lines compared to the untreated control group ($P < 0.05$). These findings suggest that IPBT effectively suppresses the proliferative capacity of cancer cells and may hold promise as a potential anticancer agent.

IPBT inhibits cell migration in the scratch assay

The effect of the IPBT derivative on cancer cell migration was evaluated using a wound healing assay (Fig. 5.1 and 5.2). The degree of wound closure was assessed at 0, 24, and 48 hours after treatment, and the remaining wound area was quantified as a percentage relative to the scratch width at 0 hours. As shown in Table 4, IPBT treatment significantly inhibited the migration of MDA-MB-231, HepG2, LNCaP, and Caco-2 cells compared to their respective control groups. The remaining wound areas in these cell lines were 91.1%, 85.8%, 109.9%, and 95.3%, respectively, while the corresponding control values were 64.0%, 94.2%, 45.0%, and 44.9% (see Fig. 5.1 and Table 4). These results indicate that IPBT treatment led to a markedly higher percentage of remaining wound area, reflecting a suppression of cell migration. Similarly, in Panc-1, HeLa, and Ishikawa cell lines, the remaining wound areas after IPBT treatment were 91.1%, 110.5%, and 127.1%, respectively, compared to 40.4%, 90.3%, and 85% in the control groups (see Fig. 5.2 and Table 4). These findings collectively demonstrate that the IPBT derivative exerts anti-migratory effects in various cancer cell lines.

Flow cytometry analysis

Apoptosis induction in the cancer cell lines MDA-MB-231, HepG2, LNCaP, Caco-2, Panc-1, HeLa, and Ishikawa were evaluated using Annexin V-FITC/PI dual staining followed by flow cytometry after treatment with the IPBT derivative at their respective EC50 concentrations for 24 hours. According to the results, the IPBT derivative induced significantly higher levels of apoptosis compared to the untreated control (Fig. 6.1 and Fig. 6.2). The percentages of apoptotic cells are presented in Table 5.

Analysis of gene expression

The effects of IPBT on the expression levels of apoptosis-related genes *BAX*, *BCL2*, *CASP3*, *CASP8*, *CASP9*, and *P53* were examined in the MDA-MB-231, HepG2, LNCaP, Caco-2, Panc-1, HeLa, and Ishikawa cell lines. RT-PCR analysis revealed that the anti-apoptotic gene *BCL2* was downregulated, with a percentage decrease observed across all cell lines. In contrast, the pro-apoptotic genes *BAX*, *CASP3*, *CASP8*, *CASP9*, and *P53* showed increased expres-

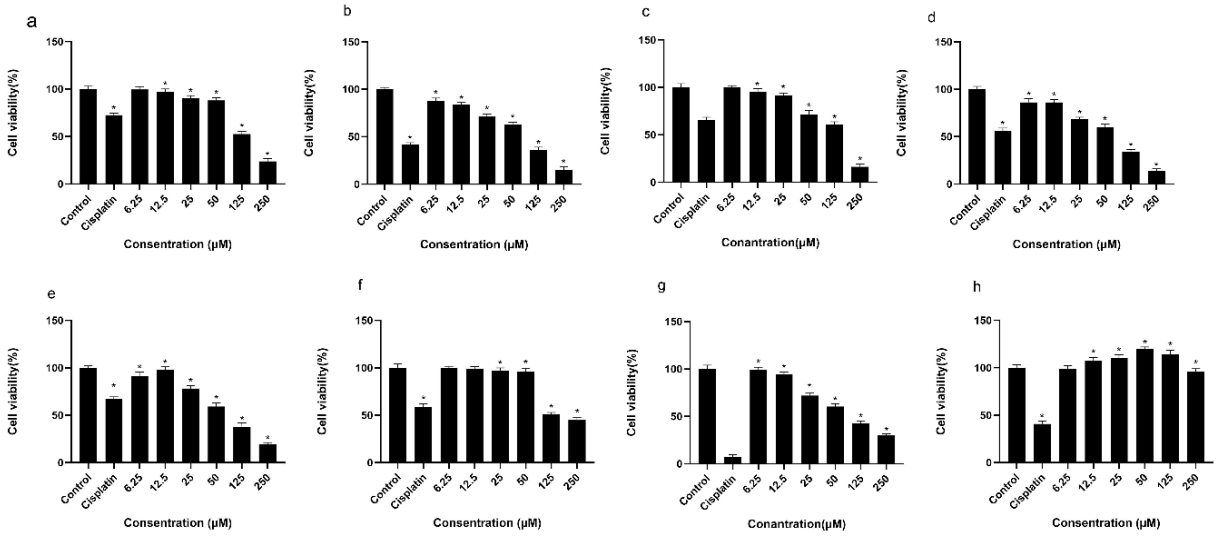

Figure 3. Cytotoxic effects of IPBT were evaluated after a 24-hour treatment in the following cell lines: (a) MDA-MB-231, (b) HepG2, (c) LNCaP, (d) Caco-2, (e) Panc-1, (f) HeLa, (g) Ishikawa, and (h) HUVEC, using the MTT assay. Cisplatin (16.5 μM) is used as a positive control. Statistical significance was determined at *$P < 0.05$.

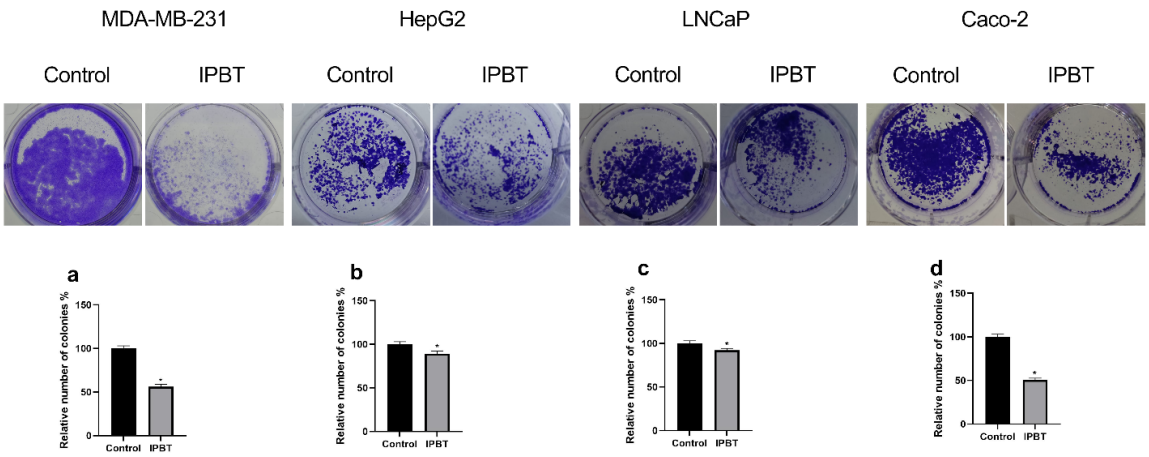

Figure 4.1. Colony formation assay results for the following cell lines: (a) MDA-MB-231, (b) HepG2, (c) LNCaP, and (d) Caco-2. Following treatment with the IPBT derivative, representative images show colonies stained with 1% crystal violet. Colony numbers were quantified based on triplicate independent experiments, and statistical significance was determined at *P < 0.05.

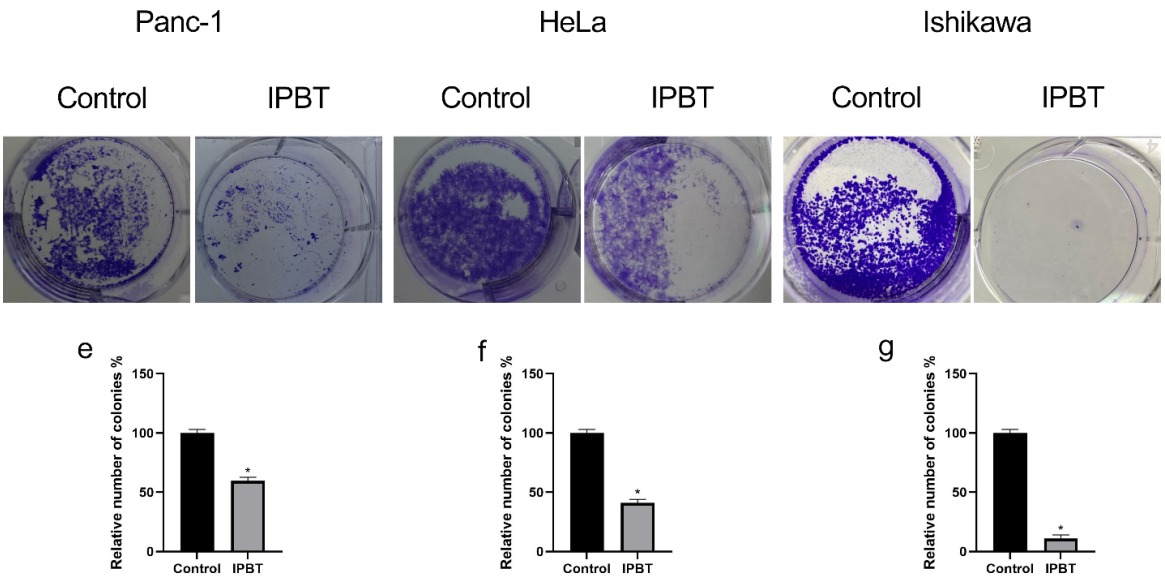

Figure 4.2. Colony formation assay results for the following cell lines: (e) Panc-1, (f) HeLa, and (g) Ishikawa. Following treatment with the IPBT derivative, representative images show colonies stained with 1% crystal violet. Colony numbers were quantified based on triplicate independent experiments, and statistical significance was determined at *P < 0.05.

sion levels (fold change) relative to the untreated control group. These results are quantitatively summarized in Table 6. and visually illustrated in Fig. 7.

Evaluation of IPBT's anti-inflammatory activity

To investigate the anti-inflammatory effects of the IPBT derivative in RAW264.7 macrophage cells, cytotoxicity was first assessed using the MTT assay after 24-hour treatment with the compound. According to the results, the IPBT derivative did not exhibit significant cytotoxic effects at concentrations ranging from 0 to 125 μM. Therefore, 125 μM was selected as the maximum concentration for subsequent anti-inflammatory analyses (Fig. 8).

To induce inflammation in RAW264.7 cells, the cells were incubated with 1 μg/mL LPS for 1 hour. Following this, the effect of the IPBT compound on nitric oxide (NO) production was evaluated by treating the LPS-induced RAW264.7 cells with 125 μM of IPBT for 24 hours. Upon analysis, the positive control (LPS) led to a 3.23-fold increase in NO levels compared to the untreated control group. Conversely,

Table 3. Percentage of colony formation in different cell lines after IPBT treatment.

Cell	MDA-MB-231	HepG2	LNCaP	Caco-2	Panc-1	HeLa	Ishikawa
Colony formation (%)	43.91	10.83	7.29	47.29	40.30	58.65	88.82

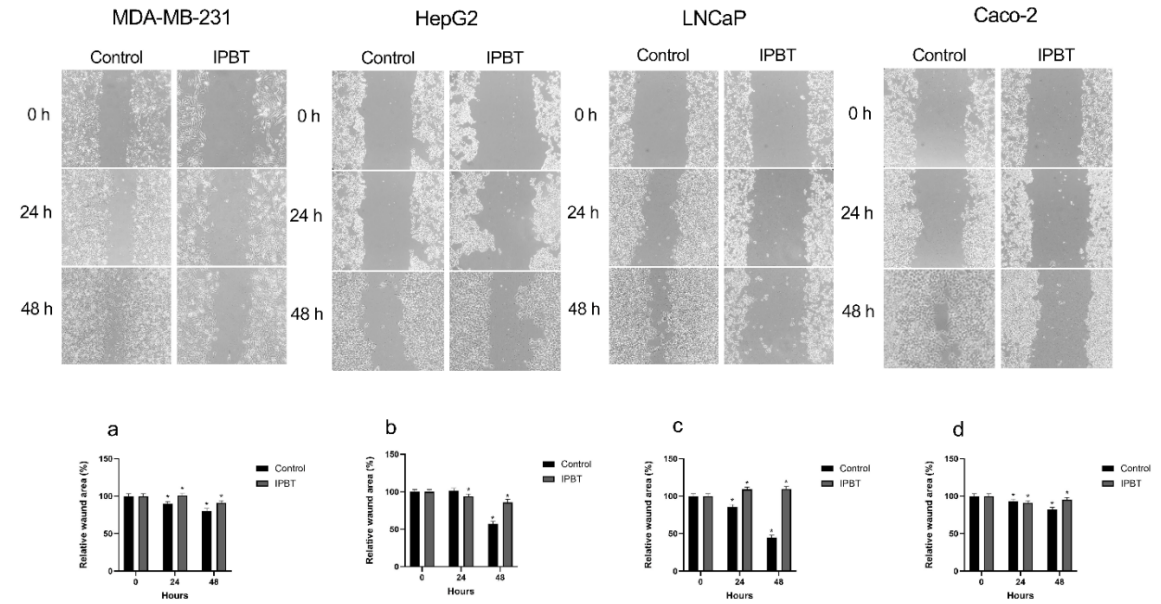

Figure 5.1. Evaluation of cell migration using the scratch (wound healing) assay in (a) MDA-MB-231, (b) HepG2, (c) LNCaP, and (d) Caco-2 cell lines. The relative scratch closure (%) was quantified based on triplicate independent experiments. Statistical significance was determined at *P < 0.05.

f5-2

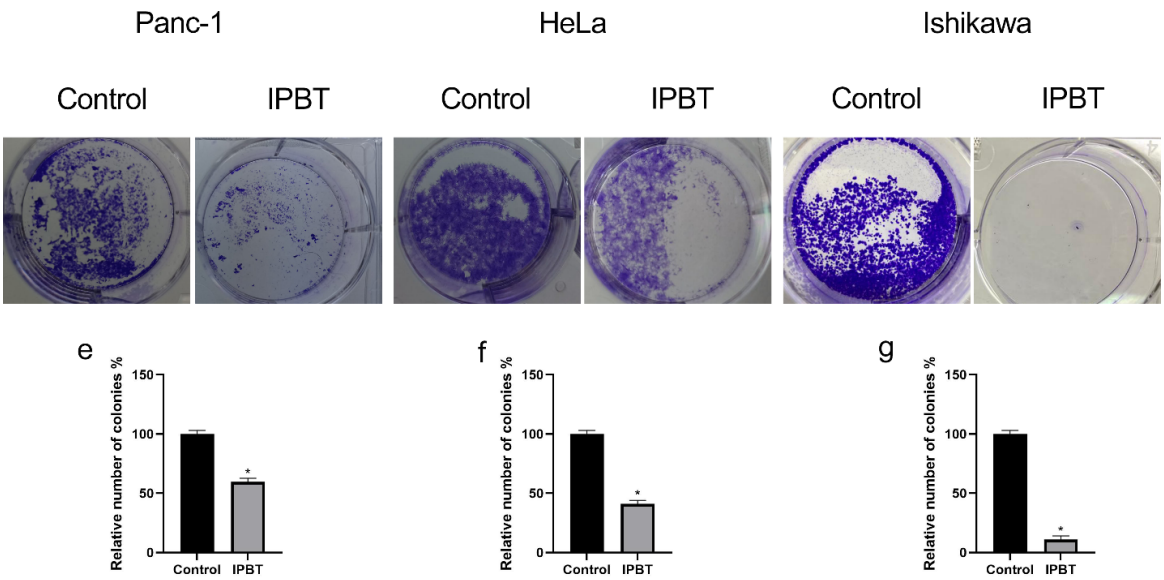

Figure 5.2. Evaluation of cell migration using the scratch (wound healing) assay in (e) PANC-1, (f) HeLa, and (g) Ishikawa cell lines. The relative scratch closure (%) was quantified based on triplicate independent experiments. Statistical significance was determined at *P < 0.05.

Table 4. Wound free area percentage in various cell lines following IPBT treatment.

Cell Line	Control (48h)	IPBT (48h)
MDA-MB-231	64.0%	91.1%
HepG2	94.2%	85.8%
LNCaP	45.0%	109.9%
Caco-2	44.9%	95.3%
Panc-1	40.4%	91.1%
HeLa	90.3%	110.5%
Ishikawa	85%	127.1%

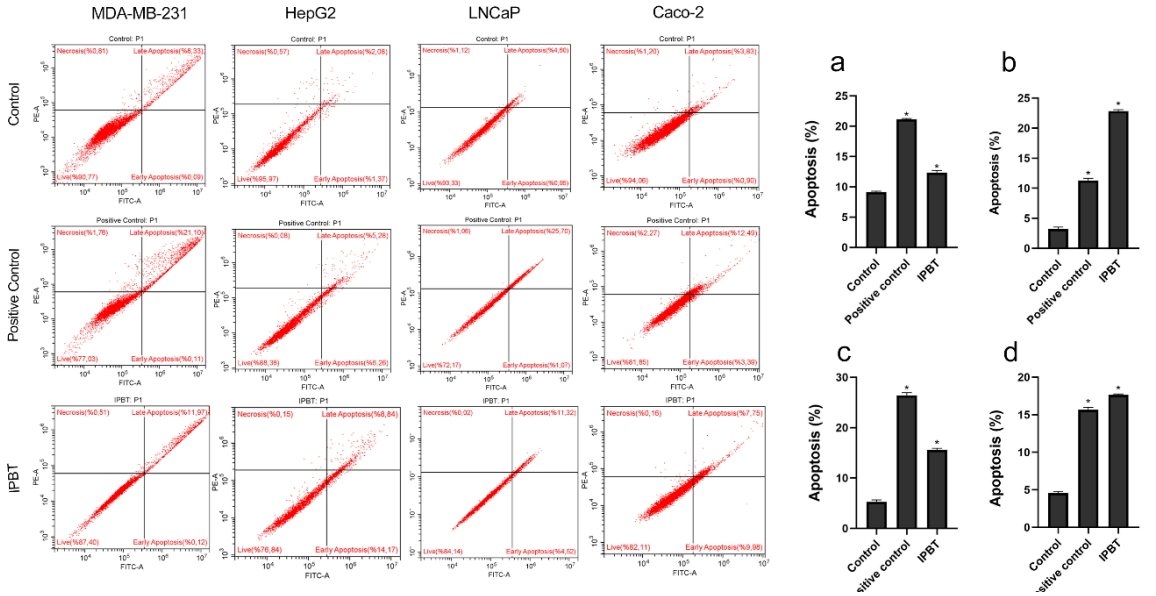

Figure 6.1. (a) MDA-MB-231, (b) HepG2, (c) LNCaP, and (d) Caco-2 cell lines after 24 hours of IPBT treatment, assessed by Annexin V-FITC/PI staining. PAX (11.4 μM) was used as the positive control. Statistical analysis was performed using one-way ANOVA. All IPBT-treated groups showed statistically significant differences compared to the control (*P $<$ 0.05, n $=$ 3).

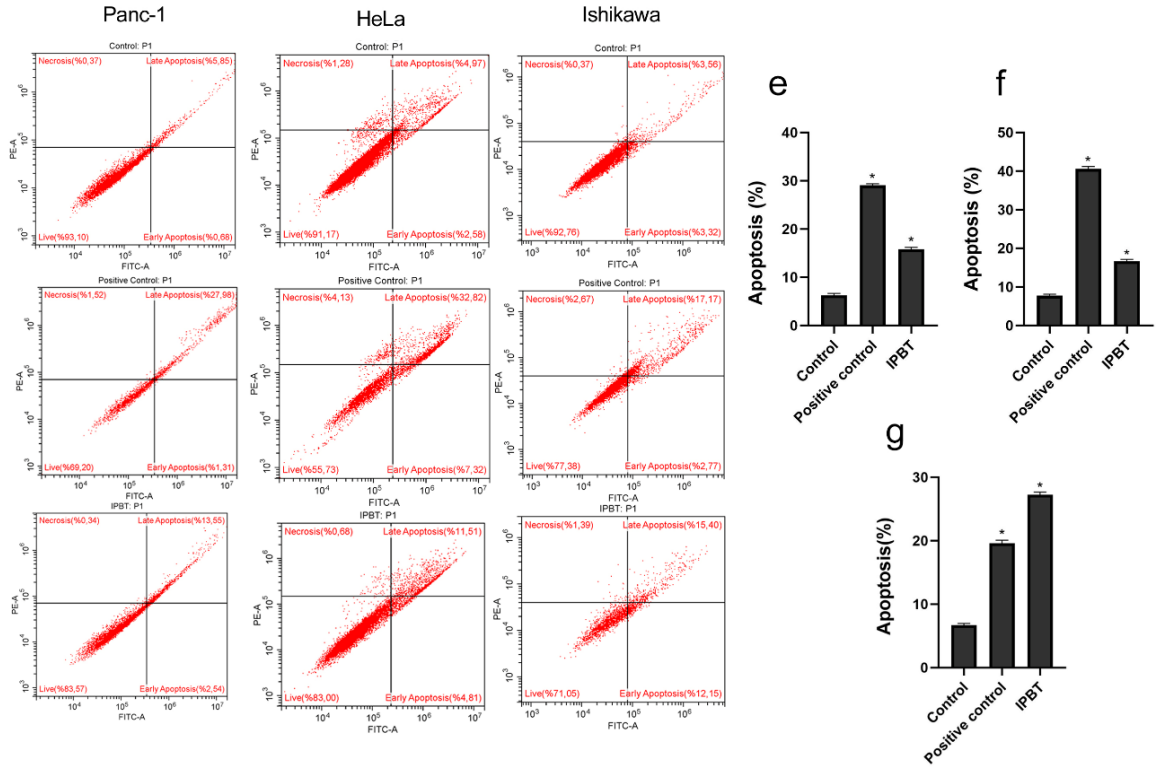

Figure 6.2. (e) PANC-1, (f) HeLa, and (g) Ishikawa cell lines after 24 hours of IPBT treatment, assessed by Annexin V-FITC/PI staining. PAX (11.4 μM) was used as the positive control. Statistical analysis was performed using one-way ANOVA. All IPBT-treated groups showed statistically significant differences compared to the control (*P $<$ 0.01, n $=$ 3).

Table 5. Apoptosis rates in various cell lines following IPBT treatment.

Cell	MDA-MB-231	HepG2	LNCaP	Caco-2	Panc-1	HeLa	Ishikawa
Control (%)	9.23	3.45	5.55	4.73	6.53	7.55	6.88
Positive Control (%)	21.21	11.54	26.8	15.88	29.29	40.14	19.94
IPBT (%)	12.09	23.01	15.84	17.73	16.09	16.32	27.55

Table 6. Comparative analysis of gene expression levels in various cell lines following IPBT treatment.

Cell	MDA-MB-231	HepG2	LNCaP	Caco-2	Panc-1	HeLa	Ishikawa
BCL2 Decrease (%)	8.93	26.54	31.22	10.18	31.93	17.35	98.48
BAX Fold Increase	2.00	4.33	13.17	3.16	3.20	7.83	21.63
CASP3 Fold Increase	13.83	4.15	3.02	2.30	3.43	3.50	3.61
CASP8 Fold Increase	10.12	4.27	3.49	1.88	4.00	8.02	11.15
CASP9 Fold Increase	8.81	1.91	1.19	1.53	1.90	2.63	4.28
P53 Fold Increase	13.64	2.60	1.26	4.56	2.53	3.58	1.89

administration of the IPBT derivative led to an approximate 48.60% decrease in NO production compared to LPS. In summary, IPBT significantly suppressed nitric oxide (NO) production in stimulated cells, indicating a strong anti-inflammatory effect (Fig. 9).

To evaluate the effects of the IPBT derivative on the mRNA expression of inflammation-related genes, RAW264.7 cells were first stimulated with LPS and then treated with 125 μM IPBT for 24 hours. Following treatment, the total RNA was isolated and reverse-transcribed into cDNA. Gene expression levels were then analyzed using qPCR. According to the results, LPS (used as a positive control) significantly improved the expression of the pro-inflammatory genes *iNOS*, *COX-2*, *IL-6*, and *TNF-*α, with fold increases of 2.02, 6.75, 2.14, and 2.76, respectively. Also, a 1.69-fold decrease in *IL-10* gene expression was observed. Treatment with the IPBT derivative markedly reduced the expression of *iNOS* (64.52%), *COX-2* (72.16%), *IL-6* (81.50%), and *TNF-*α (62.36%) compared to LPS alone. Moreover, the anti-inflammatory gene *IL-10* showed a notable increase in expression by 38.50% following IPBT treatment. These findings suggest that IPBT modulates inflammatory gene expression by downregulating pro-inflammatory markers while upregulating anti-inflammatory responses (Fig. 10).

Discussion

In this study, the anti-inflammatory and anticancer activities of the IPBT derivative including its effects on cytotoxicity, apoptosis induction, colony formation, and cell migration were evaluated. The sulfur-containing heterocyclic benzo[b]thiophene scaffold is known for its diverse pharmacological properties, particularly its ability to inhibit inflammation and cancer, and is considered a key structure in drug therapies. The present results confirm the therapeutic potential of IPBT derivative and demonstrate how these scaffolds can contribute to the advancement of research in the field of anticancer drug development. The anticancer activity of IPBT was demonstrated through cytotoxicity assays, which showed significant cytotoxic effects in cancer cells. The apoptotic mechanism of this compound can be explained by its effect on key regulators

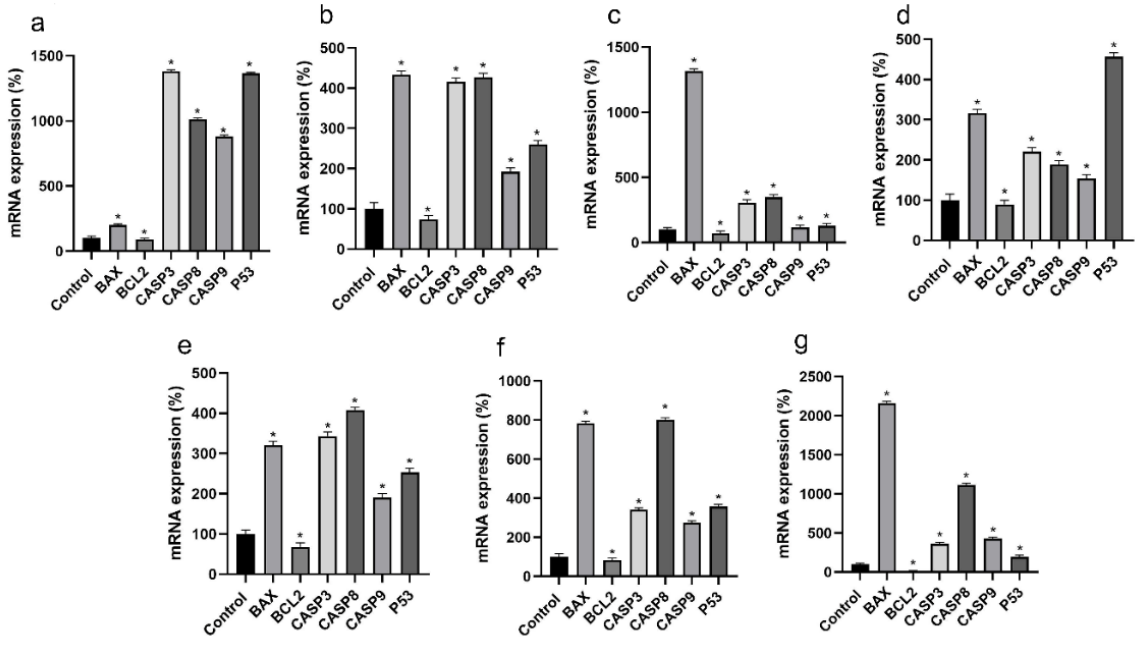

Figure 7. Relative mRNA expression levels of BAX, BCL2, CASP 3, CASP8, CASP 9, and P53 genes in different cancer cell lines: (a) MDA-MB-231, (b) HepG2, (c) LNCaP, (d) Caco-2, (e) Panc-1, (f) HeLa, and (g) Ishikawa. Statistical significance was considered at *P $<$ 0.05.

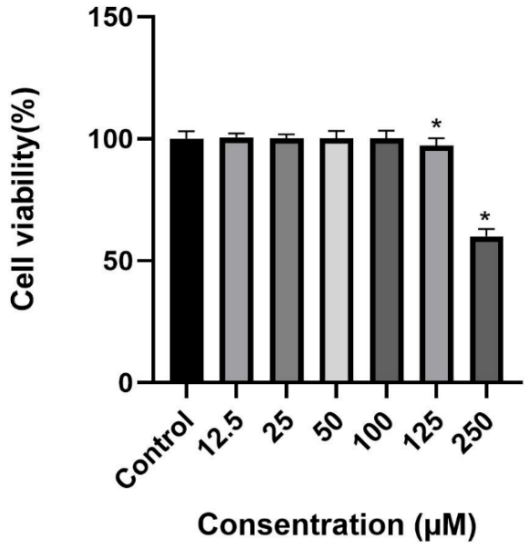

Figure 8. The cytotoxic effect of IPBT on RAW264.7 cells were evaluated after a 24-hour treatment using the MTT assay. Statistical significance was considered at *P $<$ 0.05.

of programmed cell death, particularly the *BCL2* family of gene, since decreased expression of *BCL2CASP* is known to induce apoptosis (de Vasconcelos et al., 2013; Keri et al., 2017).

Upon evaluation of our results, the IPBT derivative exhibited selective cytotoxicity against several cancer cell lines, with EC50 values of 126.67 μM for MDA-MB-231, 67.04 μM for HepG2, 127.59 μM for LNCaP, 63.74 μM for Caco-2, 76.72 μM for Panc-1, 146.75 μM for HeLa, and 110.84 μM for Ishikawa cells. Notably, the compound maintained over 50% viability in normal HUVEC cells, highlighting its selective anticancer potential (Fig. 3). Similarly, compound 17d, a benzo[b]thiophene–diarylurea derivative, demonstrated potent antiproliferative activity against HT-29 and A549 cells, with IC50 values of 5.91 μM and 14.64 μM, respectively (Zarei et al., 2020). Furthermore, a series of uridobenzothiophene derivatives were investigated as dual VEGFR/EGFR inhibitors. Most of the synthesized compounds exhibited potent cytotoxic activity against PanC-1, MCF-7, and HepG2 cell lines (El-Metwally et al., 2018). Collectively, these findings support the anticancer potential of thiophene-based compounds. In line with these results, the IPBT derivative effectively reduced the viability of various cancer cell types while sparing healthy cells, further highlighting its promise as a potential therapeutic agent.

Colony formation assays were performed to evaluate the antiproliferative effects of the IPBT compound on seven different cancer cell lines. Compared to the control group, a significant reduction in colony formation was observed following IPBT treatment. Specifically, colony formation was reduced to 43.91% in MDA-MB-231, 10.83% in HepG2, 7.29% in LNCaP, 47.29% in Caco-2, 40.30% in Panc-1, 58.65% in HeLa, and 88.82% in Ishikawa cells (Fig. 4.1, 4.2 and Table 3). These results indicate a strong suppression of long-term cell survival and anchorage-dependent growth, particularly pronounced in MDA-MB-231, HepG2, and Panc-1 cells, supporting the potent antiproliferative activity of this compound.

In a study, APTM, a thiophene derivative, significantly inhibited the proliferation of HCT116 cells as demonstrated by colony formation assays. (Kosmalski et al., 2022). Similarly, another study investigated the effect of small molecules based on benzo[b]thiophene 1,1-dioxide on colony formation in MDA-MB-231 cells. Treatment with compound 15 at concentrations of $0.5 - 6$ μM resulted in a significant reduction in clonogenic capacity (Zhang et al., 2017). Taken together, these studies reinforce the antiproliferative potential of thiophene and benzothiophene-based compounds. In this study, the effect of the IPBT derivative on cancer cell migration was examined using a wound healing assay across seven cell lines at 24 and 48 hours. As shown in Table 4, IPBT treatment significantly inhibited the migration of MDA-MB-231, HepG2, LNCaP, and Caco-2 cells compared to their respective control groups. The remaining wound areas in these cell lines were 91.1%, 85.8%, 109.9%, and 95.3%, respectively, whereas the corresponding control values were 64.0%, 94.2%, 45.0%, and 44.9% (see Fig. 5.1 and Table 4). Similarly, IPBT treatment also led to reduced migration in Panc-1, HeLa, and Ishikawa cells, with remaining wound areas of 91.1%, 110.5%, and 127.1%, respectively, compared to 40.4%, 90.3%, and 85% in the control groups (Fig. 5.2 and Table 4). Collectively, these findings demonstrate that the IPBT derivative exerts anti-migratory effects across various cancer cell lines.

These results align with previous studies reporting that thiophene-based derivatives can inhibit cancer cell migration. For example, 2-thioxothiazolidin-3-carboxylates significantly inhibited CXCL8 (interleukin-8)-induced migration via antagonism of CXCR2 in a wound healing

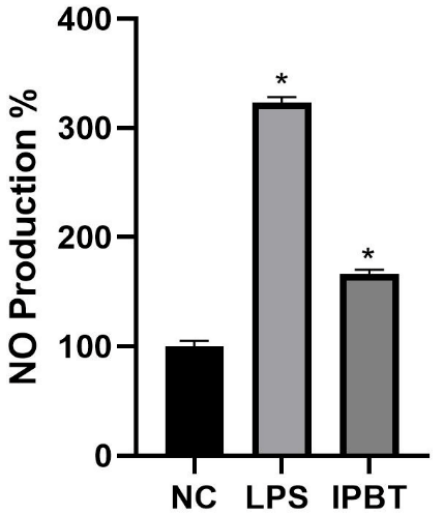

Figure 9. Effect of IPBT on nitric oxide (NO) production in RAW 264.7 cells. NO levels were measured in the culture medium of RAW 264.7 cells stimulated with LPS (1 μg/mL) following treatment with IPBT. Significance was determined at *P $<$ 0.05.

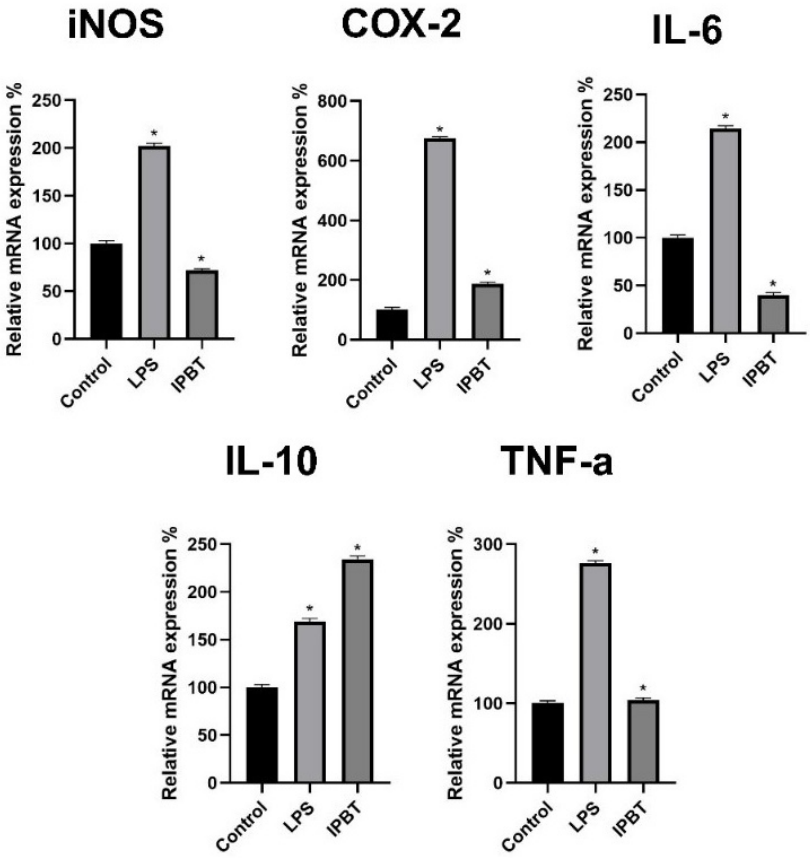

Figure 10. mRNA expression changes of iNOS, COX-2, IL-6, IL-10, and TNF-α were assessed in RAW264.7 cells relative to the control group, with statistical significance accepted at *P $<$ 0.05.

assay (Xue et al., 2020). Similarly, thiophene[3,2-d] pyrimidine tubulin inhibitors showed potent inhibition of melanoma cell migration, with compound 5c demonstrating significant effects in a wound healing assay (Caro et al., 2020). Additionally, a benzothiazole derivative, *N*-formyl-2-(5-nitrothiophen-2-yl) benzothiazole-6-carbohydrazide, significantly inhibited prostate cancer cell migration in a scratch-wound healing assay (Rodrigues et al., 2013). Together, these findings support the anti-migratory potential of IPBT and highlight the therapeutic promise of thiophene-based compounds.

In the current study, the apoptotic potential of the IPBT derivative was evaluated in seven different human cancer cell lines. Compared with their respective control groups, a significant increase in the population of apoptotic cells was observed following IPBT treatment. The apoptosis rate increased from 9.23% to 12.09% in MDA-MB-231, 3.45% to 23.01% in HepG2, 5.55% to 15.84% in LNCaP, 4.73% to 17.73% in Caco-2, 6.53% to 16.09% in Panc-1, 7.55% to 16.32% in HeLa, and 6.88% to 27.55% in Ishikawa cells. These results confirm that IPBT effectively induces apoptosis in multiple cancer cell lines.

To explore the underlying molecular mechanisms, quantitative RT-PCR analysis was performed. A consistent downregulation of the anti-apoptotic gene *BCL2* was observed in MDA-MB-231 (8.93%), HepG2 (26.54%), LNCaP (31.22%), Caco-2 (10.18%), Panc-1 (31.93%), HeLa (17.35%), and Ishikawa (98.48%) cells. In contrast, pro-apoptotic genes including *BAX*, *CASP3*, *CASP8*, *CASP9*, and *P53* were significantly upregulated, indicating activation of both intrinsic (mitochondrial) and extrinsic apoptotic pathways (Fig. 4.1, 4.2 and Table 3).

Further research revealed that compound 8b, a benzo[b]thiophene 1,1–dioxide derivative, effectively induced apoptosis in cancer cells, accompanied by decreased intracellular ROS levels and loss of mitochondrial membrane potential, suggesting activation of the intrinsic apoptotic pathway (Romagnoli et al., 2021). Another study found that the thiophene derivative 2-bromo-5-(2-(methylthio) phenyl) thiophene significantly altered *CASP3*, *BCL2*, and Bax levels, indicating apoptosis induction (Li et al., 2021). In another study, the tetrahydrobenzo[b]thiophene compound BU17 induced G2/M phase arrest and significantly increased *CASP3* and *CASP9* levels (Abdel-Rahman et al., 2021). Collectively, these findings indicate that IPBT induces apoptosis through mechanisms consistent with those of structurally related compounds, highlighting its strong therapeutic potential, particularly in cancers characterized by resistance to apoptosis.

Finally, the anti-inflammatory properties of IPBT were investigated in RAW264.7 macrophage cells by evaluating nitric oxide (NO) production and cytotoxicity following lipopolysaccharide (LPS) stimulation using the MTT assay. RAW264.7 cells pretreated with 125 μM IPBT one hour after LPS exposure showed a significant reduction in

LPS-induced NO production. IPBT treatment reduced nitrite accumulation by approximately 48.60% after 24 hours, whereas LPS stimulation alone increased NO levels 3.23-fold compared to the untreated control group (Fig. 9). Gene expression analysis further supported these findings by revealing a marked downregulation of key pro-inflammatory mediators: Inducible nitric oxide synthase (*iNOS*) by 64.52%, cyclooxygenase-2 (*COX-2*) by 72.16%, interleukin-6 (*IL-6*) by 81.50%, and tumor necrosis factor-alpha (*TNF-*α) by 62.36%. In contrast, expression of the anti-inflammatory cytokine interleukin-10 (*IL-10*) was upregulated by 38.50% (Fig. 10).

In line with our findings, previous studies have reported similar anti-inflammatory effects of benzothiophene and tetrahydrobenzothiophene derivatives. Newly synthesized 2-amino-4,5,6,7-tetrahydrobenzo[b]thiophene derivatives were identified as NRF2 activators, demonstrating potent anti-inflammatory activity by inhibiting NO production and suppressing proinflammatory cytokines in LPS-stimulated RAW264.7 macrophages (Maka et al., 2022). Similarly, a separate study evaluated a series of 2-phenyl-4,5,6,7-tetrahydrobenzothiophene derivatives for their in vitro *COX* inhibitory potential. Compounds 4j, 4k, and 4q exhibited high selectivity toward *COX-2* and showed anti-inflammatory efficacy comparable to celecoxib (Khatri et al., 2017). In another study, thiophene derivatives demonstrated strong anti-inflammatory activity, surpassing conventional NSAIDs in in vitro, in silico, and in vivo assays (Cruz et al., 2021).

These results suggest that IPBT, consistent with structurally related benzothiophene derivatives, may exert its anti-inflammatory effects through suppression of pro-inflammatory gene expression and upregulation of anti-inflammatory mediators, highlighting its therapeutic potential in inflammatory conditions.

Conclusion

The comprehensive in vitro results presented in this study indicate that IPBT is a promising compound for further development of anticancer drugs. Its potent anticancer and anti-inflammatory properties are supported by selective cytotoxicity, induction of apoptosis, and inhibition of cancer cell migration. Based on the research results, IPBT appears to be a potential lead compound. However, further research is required to fully elucidate the underlying mechanisms of action and to optimize the compound's molecular structure for enhanced therapeutic efficacy and effectiveness.

Method

Chemical reagent: 3-iodo-2-phenylbenzo[b]thiophene (IPBT)

To the solution of the compound methyl(2-(phenylethynyl) phenyl) (3) sulfane (224 mg, 1 mmol) in CH_2Cl_2 (5 mL), I_2 (761 mg, 3 mmol) was added and stirred at room temperature for 120 min. Then, saturated sodium thiosulfate ($Na_2S_2O_3$) solution was added to the reaction mixture and extracted with EtOAc. The combined organic extracts were dried with anhydrous $MgSO_4$. After filtration and removal of solvent, the residue was purified by column chromatography to obtain compound IPBT (98% yield) as a white solid. 1H NMR (400 MHz, $CDCl_3$) δ 7.88 (d, $J = 8.5$ Hz, 1H), 7.82 (d, $J = 8$ Hz, 1H), $7.76 - 7.71$ (m, 2H), $7.55 - 7.45$ (m, 4H), 7.42 (dt, $J = 8.5$, 1.2 Hz, 1H). 13C NMR (100 MHz, $CDCl_3$) δ 142.1, 141.9, 138.9, 134.6, 130.08, 128.9, 128.5, 126.3, 125.5, 125.4, 122.1, 79.5. HRMS calculated: C14H9SI, 335.9481; found: 335.9470 (Fig. S1-4).

ADME/T analysis

To obtain the pharmacokinetic properties of the synthesized derivative, ADME/T (absorption, distribution, metabolism, elimination and toxicity) analysis was performed using SwissADME software (Deng et al., 2022). In silico results were presented on the drug application of the tested derivative, its passage through the gastrointestinal tract (GI), blood-brain barrier (BBB) as well as transport via P-glycoprotein (P-gp) based on the SwissADME in-house radar and toxicity prediction models.

Cell cultivation and cytotoxicity assessment

MDA-MB-231 (human breast adenocarcinoma), HepG2 (human hepatocellular carcinoma), LNCaP (human prostate adenocarcinoma), Caco-2 (human colorectal adenocarcinoma), Panc-1 (human pancreatic carcinoma), HeLa (cervimetric Ad), HUVEC (human umbilical vein endothelial cells), and RAW 264.7 (mouse macrophages) cells were purchased from the Europeopean Collection of Cell Culture of Cell Cultures (ECACCCC).

In this study, MDA-MB-231, HepG2, Caco-2, HeLa, and Ishikawa cells were maintained in Dulbecco's Modified Eagle Medium (DMEM, Gibco), while LNCaP and Panc-1 cells were cultured in RPMI-1640 medium (Gibco). All media were supplemented with 10% heat-inactivated fetal bovine serum (FBS, Capricorn) and 1% penicillin-streptomycin solution (Capricorn). Cells were incubated at 37 °C in a humidified atmosphere containing 5% CO_2 as previously described (Aguiar et al., 2016; Banerjee et al., 2019).

Cells were plated at a density of 2×10^3 cells per well and then treated with different concentrations (0, 6.25, 12.5, 25, 50, 125, and 250 μM) of IPBT derivative for 24 h. After treatment the medium was removed, and refreshed with medium containing MTT solution (0.5 mg/mL) and incubated for 4 h in under standard incubation conditions (Kouhestani et al., 2018). The medium was then removed, and dimethyl sulfoxide (DMSO, Carlo Erba) was added to each well to dissolve the formed formazan crystals. The absorbance was measured at 590 nm using a microplate reader (Epoch, BioTek). The EC50 value was calculated using GraphPad Prism version 10 (GraphPad Software, CA).

Colony forming ability analysis

Cells were seeded at a density of 1×10^3 cells per well in 6-well plates, and the colony formation assay was performed as previously described (Liao et al., 2018). Cells were incubated with the EC50 concentration of the IPBT compound for 24 h. Then the culture media was refreshed, and the cells were maintained for $1 - 2$ weeks to allow colony formation. Subsequently, the cells were washed

with phosphate-buffered saline (PBS; Gibco) and fixed with 100% methanol (Isolab) for 20 min at −20 °C. Cells were then stained with 0.1% crystal violet (Merck) at room temperature for 15 min. After staining, the cells were washed $2-3$ times with PBS and imaged. Colony numbers were quantified using ImageJ software version 1.6 (USA).

Wound healing assay

To assess the effect of the IPBT derivative on cell migration, a wound healing assay was carried out following a previously established protocol (Mutlu et al., 2022). Briefly, cancer cells (3×10^4 per well) were seeded into 6-well plates and incubated for 24 hours to allow for monolayer formation. A straight scratch was then introduced across the cell layer using a sterile 200 μL pipette tip, followed by washing with 1X PBS to remove debris. Cells were subsequently exposed to the EC50 concentration of the IPBT compound for 24 hours. After treatment, the medium was replaced with fresh culture medium, and wound closure was monitored at 0, 24, and 48 hours using a 10× objective on an inverted microscope. The extent of cell migration into the wound area was quantified using ImageJ software (version 1.6).

Apoptosis detection

Apoptotic cell death was evaluated using the Annexin V-FITC apoptosis detection kit (Elabscience), in accordance with the manufacturer's guidelines and previously published protocols (Elmongy et al., 2022). Cancer cells were cultured in 6-well plates at a density of 3×10^4 cells per well. Following a 24-hour exposure to the EC_{50} concentration of the IPBT compound, cells were collected and centrifuged at 2000 rpm for 5 minutes. The cell pellet was then resuspended in 1X Annexin binding buffer and incubated with Annexin V-FITC and propidium iodide (PI) for staining. Subsequently, cell populations including viable, apoptotic, and necrotic cells were analyzed using flow cytometry (CytoFLEX, Beckman Coulter).

Isolation of RNA, cDNA synthesis, and quantitative RT-PCR analysis

Total RNA was isolated from the cultured cells using the GeneAll® Hybrid-R RNA Isolation Kit in accordance with the manufacturer's instructions. The synthesis of complementary DNA (cDNA) was performed using the A.B.T. cDNA synthesis kit, which includes an RNase inhibitor to protect RNA integrity. Quantitative real-time PCR (qRT-PCR) was then carried out using the StepOnePlus™ Real-Time PCR System (Applied Biosystems™, Thermo Fisher Scientific, USA) to evaluate the mRNA expression levels of *P53*, *BAX*, *BCL2*, *CASP3*, *CASP8*, and *CASP9*, following the procedure described in a previous study (Yılmaz et al., 2022). β-actin served as the housekeeping gene for normalization. The primer sequences used for amplification are presented in Table 7.

Determination of Nitric Oxide production

Nitric Oxide (NO) production was measured according to the Griess method, as previously described (Griess, 1879). RAW 264.7 cells were cultured in DMEM medium without phenol red and supplemented with IPBT at various concentrations (0, 6.25, 12.5, 25, 50, 125 and 250 μM). After 24 h, 100 μL of Grice reagent (Merck Millipore) was added to 100 μL of culture medium per well in a 96-well plate and incubated for 10 min in the dark at room temperature. The absorbance of the samples was then measured at 540 nm using a microplate reader (Epoch BioTek).

Table 7. RT-qPCR primer sequences for target genes in IPBT experiments.

Gene	Forward Primer	Reverse Primer
β-actin	CACCATTGGCAATGAGCGGTTC	AGGTCTTTGCGGATGTCCACGT
P53	CCTCAGCATCTTATCCGAGTGG	TGGATGGTGGTACAGTCAGAGC
BAX	TCAGGATGCGTCCACCAAGAAG	TGTGTCCACGGCGGCAATCATC
BCL2	ATCGCCCTGTGGATGACTGAGT	GCCAGGAGAAATCAAACAGAGGC
CASP3	GGAAGCGAATCAATGGACTCTGG	GCATCGACATCTGTACCAGACC
CASP8	AGAAGAGGGTCATCCTGGGAGA	TCAGGACTTCCTTCAAGGCTGC
CASP9	GTTTGAGGACCTTCGACCAGCT	CAACGTACCAGGAGCCACTCTT

Table 8. Sequences of primers employed in qRT-PCR for inflammatory gene assay.

Gene	Forward Primer	Reverse Primer
GAPDH	CATCACTGCCACCCAGAAGACTG	ATGCCAGTGAGCTTCCCGTTCAG
COX-2	GCGACATACTCAAGCAGGAGCA	AGTGGTAACCGCTCAGGTGTTG
iNOS	GAGACAGGGAAGTCTGAAGCAC	CCAGCAGTAGTTGCTCCTCTTC
IL-6	TGGACCTTCCAGGATGAGGACA	GTTCATCTCGGAGCCTGTAGTG
IL-10	CGGGAAGACAATAACTGCACCC	CGGTTAGCAGTATGTTGTCCAGC
TNF-α	GGTGCCTATGTCTCAGCCTCTT	GCCATAGAACTGATGAGAGGGAG

Analysis of inflammatory gene expression

The mRNA expression levels of inflammation-related genes were determined according to the RT-PCR method described in the previous sections. The GAPDH gene was used as a housekeeping gene to normalize and evaluate the relative expression of *COX-2*, *iNOS*, *IL-6*, *IL-10*, and *TNF-α* genes. The sequences of the primers used in this study are presented in Table 8.

Statistical analysis

Statistical analysis of the dose and control group comparisons was performed using GraphPad Prism software version 10. In all analyses, a p value of less than 0.05 was considered as the level of statistical significance. In RT-PCR data analysis, gene expression quantification was performed using the 2^ΔΔCT method.

Acknowledgment

This study was supported by Pamukkale University Scientific Research Projects Commission (Project No: 2023FEBE015).

Authors contributions
Authors have contributed equally in preparing and writing the manuscript.

Availability of data and materials
The data that support the findings of this study are available from the corresponding author, upon reasonable request.

Conflict of interests
The authors declare that they have no known competing financial interests or personal relationships that could have appeared to influence the work reported in this paper.

References

Abdel-Rahman, S. A., Wafa, E. I., Ebeid, K., Geary, S. M., Naguib, Y. W., El-Damasy, A. K., & Salem, A. K. (2021). "Thiophene derivative-loaded nanoparticles mediate anticancer activity through the inhibition of kinases and microtubule assembly". *Adv. Drug Deliv. Rev.*, ***170***, 1–10. https://doi.org/10.1002/adtp.202100058

Aguiar, A. C. V., Moura, R. O., Mendonça Junior, J. F. B., Rocha, H. A. O., Câmara, R. B. G., & Schiavon, M. S. C. (2016). Evaluation of the antiproliferative activity of 2-amino thiophene derivatives against human cancer cell lines. *Biomedicine and Pharmacotherapy*, *84*, 403–414. https://doi.org/10.1016/j.biopha.2016.09.026

Archna, A., Pathania, S., & Chawla, P. A. (2020). "Thiophene-based derivatives as anticancer agents: an overview on decade's work". *Bioorg. Chem.*, ***101***, 104026. https://doi.org/10.1016/j.bioorg.2020.104026

Banerjee, K., Rai, V. R., & Umashankar, M. (2019). Effect of peptide-conjugated nanoparticles on cell lines. *Progress in Biomaterials*, *8*, 11–21. https://doi.org/10.1007/s40204-019-0106-9

Cao, W., Chen, H.-D., Yu, Y.-W., Li, N., & Chen, W.-Q. (2015). "Changing profiles of cancer burden worldwide and in China: a secondary analysis of the global cancer statistics 2020 ". *Chin. Med. J.*, ***134***(7), 783–791. https://doi.org/10.1097/CM9.0000000000001474

Caro, D., Rivera, D., Ocampo, Y., Müller, K., & Franco, L. A. (2020). A promising naphthoquinone [8-hydroxy-2-(2-thienylcarbonyl)naphtho[2,3-b]thiophene-4,9-dione] exerts anti-colorectal cancer activity through ferroptosis and inhibition of mapk signaling pathway based on rna sequencing. *Open Chemistry*, *18*, 1242–1255. https://doi.org/10.1515/chem-2020-0170

Cruz, R. M. D., Mendonça-Junior, F. J. B., de Mélo, N. B., Scotti, L., de Araújo, R. S. A., de Almeida, R. N., & de Moura, R. O. (2021). "Thiophene-based compounds with potential anti-inflammatory activity". *Pharmaceutics*, ***14***(7), 692. https://doi.org/10.3390/ph14070692

Debela, D. T., Muzazu, S. G. Y., & Manyazewal, T. (2021). "New approaches and procedures for cancer treatment: current perspectives". *SAGE Open Med.*, ***9***(4). https://doi.org/10.1177/20503121211034366

Deng, Q., Gu, J., Zhang, H., Zhang, Y., & Meng, X. (2022). Sustainable access to benzothiophene derivatives bearing a trifluoromethyl group via a three-component domino reaction in water. *Organic and Biomolecular Chemistry*, *20*, 6611–6619. https://doi.org/10.1039/D2OB01034H

de Vasconcelos, A., Campos, V. F., Nedel, F., Seixas, F. K., Dellagostin, O. A., Smith, K. R., & Pereira de Pereira, C. M. (2013). "Cytotoxic and apoptotic effects of chalcone derivatives of 2-acetyl thiophene on human colon adenocarcinoma cells". *Cell Biochem. Funct.*, ***31***(4), 289–297. https://doi.org/10.1002/cbf.2897

El-Metwally, S. A., Khalil, A. K., El-Naggar, A. M., & El-Sayed, W. M. (2018). Novel tetrahydrobenzo[b]thiophene compounds exhibit anticancer activity through enhancing apoptosis and inhibiting tyrosine kinase. *Anti-Cancer Agents in Medicinal Chemistry*, *18*(12), 1761–1769. https://doi.org/10.2174/1871520618666180813120558

Elmongy, E. I., Attallah, N. G. M., Altwaijry, N., AlKahtani, M. M., & Henidi, H. A. (2022). Design and synthesis of new thiophene/thieno[2,3-d]pyrimidines along with their cytotoxic biological evaluation as tyrosine kinase inhibitors in addition to their apoptotic and autophagic induction. *Molecules*, *27*(1), 123. https://doi.org/10.3390/molecules27010123

Fakhr, I. M. I., Radwan, M. A. A., El-Batran, S., Abd El-Salam, O. M. E., & El-Shenawy, S. M. (2009). "Synthesis and pharmacological evaluation of 2-substituted benzo[b]thiophenes as anti-inflammatory and analgesic agents". *Eur. J. Med. Chem.*, ***44***(4), 1718–1725. https://doi.org/10.1016/j.ejmech.2008.02.034

Gad, E. M., Nafie, M. S., Eltamany, E. H., Hammad, M. S. A. G., Barakat, A., & Boraei, A. T. A. (2020). Discovery of new apoptosis-inducing agents for breast cancer based on ethyl 2-amino-4,5,6,7-tetrahydrobenzo[b]thiophene-3-carboxylate: Synthesis, in vitro, and in vivo activity evaluation. *Molecules*, *25*(11), 2523. https://doi.org/10.3390/molecules25112523

Griess, P. (1879). "Bemerkungen zu der Abhandlung der HH. Weselsky und Benedikt Ueber einige Azoverbindungen. Ber". *Dtsch. Chem. Ges.*, ***12***, 426–428. https://doi.org/10.1002/cber.187901201117

Haberkorn, U. (2007). "What is cancer? In: Advances in Nuclear Oncology, 1st ed". *CRC Press*, 1–16. https://doi.org/10.3109/9781420091380-5

Hanahan, H., & Weinberg, R. A. (2011). "Hallmarks of cancer: the next generation". *Cell*, ***144***(5), 646–674. https://doi.org/10.1016/j.cell.2011.02.013

Haridevamuthu, B., Manjunathan, T., Guru, A., Kumar, R. S., Rajagopal, R., Kuppusamy, P., Juliet, A., Gopinath, P., & Arockiaraj, J. (2022). Hydroxyl containing benzo[b]thiophene analogs mitigates the acrylamide induced oxidative stress in the zebrafish larvae by stabilizing the glutathione redox cycle. *Life Sciences*, *298*, 120507. https://doi.org/10.1016/j.lfs.2022.120507

Hegde, P. S., & Chen, D. S. (2020). "Top 10 challenges in cancer immunotherapy". *Cancer Immunol. Res.*, ***52***(1), 17–35.

Hiremath, C. G., Heggnnavar, G. B., Karidurganavar, M. Y., & Hiremath, M. B. (2019). Co-delivery of paclitaxel and curcumin to folate-positive cancer cells using pluronic-coated iron oxide nanoparticles. *Progress in Biomaterials*, *8*, 155–168. https://doi.org/10.1007/s40204-019-0118-5

Kalaria, P. N., Karad, S. C., & Raval, D. K. (2018). A review on diverse heterocyclic compounds as the privileged scaffolds in antimalarial drug discovery. *European Journal of Medicinal Chemistry*, *158*, 917–936. https://doi.org/10.1016/j.ejmech.2018.08.040

Keri, R. S., Chand, K., Budagumpi, S., Somappa, S. B., Patil, S. A., & Nagaraja, B. M. (2017). "An overview of benzo[b]thiophene-based medicinal chemistry". *Eur. J. Med. Chem.*, ***138***, 1002–1033. https://doi.org/10.1016/j.ejmech.2017.07.038

Khatri, C. K., Indalkar, K. S., Patil, C. R., Goyal, S. N., & Chaturbhuj, G. U. (2017). Novel 2-phenyl-4,5,6,7-tetrahydro[b]benzothiophene analogues as selective cox-2 inhibitors: Design, synthesis, anti-inflammatory evaluation, and molecular docking studies. *"Bioorg. Med. Chem. Lett."*, ***27***(8), 1721–1726. https://doi.org/10.1016/j.bmcl.2017.02.076

Kosmalski, T., Hetmann, A., Studzińska, R., Baumgart, S., Kupczyk, D., & Roszek, K. (2022). The oxime ethers with heterocyclic, alicyclic and aromatic moiety as potential anti-cancer agents. *Molecules*, *27*(4), 1374. https://doi.org/10.3390/molecules27041374

Kouhestani, F., Dehabadi, F., Shahriari, M. H., & Motamedian, S. R. (2018). Allogenic vs. synthetic granules for bone tissue engineering: An in vitro study. *Progress in Biomaterials*, *7*, 133–141. https://doi.org/10.1007/s40204-018-0092-3

Li, W.-Z., Xi, H.-Z., Wang, Y.-J., Ma, H.-B., Cheng, Z.-Q., Yang, Y., Wu, M.-L., Liu, T.-M., Yang, W., Wang, Q., Liao, M.-Y., Zhang, Y.-W., & Xia, Y. (2021). Design, synthesis, and biological evaluation of benzo[b]thiophene 1,1-dioxide derivatives as potent stat3 inhibitors. *Chemistry and Biology of Drug Design*, *98*(5), 835–849. https://doi.org/10.1111/cbdd.13939

Liao, X., Huang, J., Lin, W., Long, Z., Xie, Y., & Ma, W. (2018). Aptm, a thiophene heterocyclic compound, inhibits human colon cancer hct116 cell proliferation through p53-dependent induction of apoptosis. *DNA and Cell Biology*, *37*(2), 119–128. https://doi.org/10.1089/dna.2017.3962

Ma, X., & Yu, H. (2007). "Global burden of cancer". *Yale J. Biol. Med.*, ***79***(3-4), 85–94.

Mabkhot, Y. N., Kaal, N. A., Alterary, S., Mubarak, M. S., Alsayari, A., & Muhsinah, A. B. (2019). "New thiophene derivatives as antimicrobial agents". *J. Heterocycl. Chem.*, ***56***(10), 2845–2953. https://doi.org/10.1002/jhet.3688

Maka, K. K., Shiminga, Z., Epemolud, O., Dinkova-Kostova, A. T., Wells, G., Gazaryan, I. G., Sakirollak, R., Mohd, Z., & Pichika, M. R. (2022). "Synthesis and anti-inflammatory activity of novel 2-amino-4,5,6,7-tetrahydrobenzo[b]thiophene-derived NRF2 activators". *Preprint*, https://doi.org/10.2139/ssrn.4097876

Mishra, R., Kumar, N., Mishra, I., & Sachan, N. (2020). "A review on anticancer activities of thiophene and its analogs". *Mini Rev. Med. Chem.*, ***20***(19), 1944–1965. https://doi.org/10.2174/1389557520666200715104555

Mutlu, D., Cakir, C., Ozturk, M., & Arslan, S. (2022). "Anticancer and apoptotic effects of a polysaccharide extract isolated from Lactarius chrysorrheus Fr. in HepG2 and PANC-1 cell lines ". *Arch. Biol. Sci.*, ***74***, 315–324. https://doi.org/10.2298/ABS220803030M

Nie, Q., Hu, Y., Yu, X., Li, X., & Fang, X. (2022). Induction and application of ferroptosis in cancer therapy. *Cancer Cell International*, *22*, 12. https://doi.org/10.1186/s12935-021-02366-0

Pedraza-Fariña, L. G. (2007). "Mechanisms of oncogenic cooperation in cancer initiation and metastasis". *Yale J. Biol. Med.*, ***79***(3-4), 95–103.

Pucci, C., Martinelli, G., & Ciofani, G. (2019). "Innovative approaches for cancer treatment: current perspectives and new challenges". *Ecancermedicalscience*, ***13***, 961. https://doi.org/10.3332/ecancer.2019.961

Qadir, T., Amin, A., Sharma, P. K., Jeelani, I., & Abe, H. (2022). A review on medicinally important heterocyclic compounds. *Open Medicinal Chemistry Journal*, *16*, e2202280. https://doi.org/10.2174/18741045-v16-e2202280

Rodrigues, J. R., Charris, J., Camacho, J., Barazarte, A., Gamboa, N., Nitzsche, B., Höpfner, M., Lein, M., Jung, K., & Abramjuk, C. (2013). N-formyl-2-(5-nitrothiophen-2-yl) benzothiazole-6-carbohydrazide as a potential anti-tumour agent for prostate cancer in experimental studies. *Journal of Pharmacy and Pharmacology*, *65*(3), 411–422. https://doi.org/10.1111/j.2042-7158.2012.01607.x

Romagnoli, R., Preti, D., Hamel, E., Bortolozzi, R., Viola, G., Brancale, A., Ferla, S., Morciano, G., & Pinton, P. (2021). "Concise synthesis and biological evaluation of 2-aryl-3-anilinobenzo[b]thiophene derivatives as potent apoptosis-inducing agents ". *Bioorg. Chem.*, ***112***, 104919. https://doi.org/10.1016/j.bioorg.2021.104919

Rosada, B., Bekier, A., Cytarska, J., Płaziński, W., Zavyalova, O., Sikora, A., Dzitko, K., & Łaczkowski, K. Z. (2019). Benzo[b]thiophene-thiazoles as potent anti-toxoplasma gondii agents: Design, synthesis, tyrosinase/tyrosine hydroxylase inhibitors, molecular docking study, and antioxidant activity. *European Journal of Medicinal Chemistry*, *184*, 111765. https://doi.org/10.1016/j.ejmech.2019.111765

Shah, R., & Verma, P. K. (2019). "Synthesis of thiophene derivatives and their anti-microbial, antioxidant, anticorrosion and anticancer activity". *BMC Chem.*, ***13***(54). https://doi.org/10.1186/s13065-019-0569-8

Singh, A., Singh, G., & Bedi, P. M. S. (2020). Thiophene derivatives: A potent multitargeted pharmacological scaffold. *Journal of Heterocyclic Chemistry*, *57*(7), 2658–2703. https://doi.org/10.1002/jhet.3990

Sung, H., Ferlay, J., Siegel, R. L., Laversanne, M., Soerjomataram, I., Jemal, A., & Bray, F. (2021). "Global cancer statistics 2020: GLOBOCAN estimates of incidence and mortality worldwide for 36 cancers in 185 countries". *CA Cancer J. Clin.*, ***71***(3), 209–249. https://doi.org/10.3322/caac.21660

Xue, D., Chen, W., & Neamati, N. (2020). "Discovery, structure-activity relationship study and biological evaluation of 2-thioureidothiophene-3-carboxylates as a novel class of C-X-C chemokine receptor 2 (CXCR2) antagonists". *Eur. J. Med. Chem.*, ***204***, 112387. https://doi.org/10.1016/j.ejmech.2020.112387

Yılmaz, C., Pirdawid, A. O., Babat, C. F., Konuş, M., Çetin, D., Kıvrak, A., Algso, M. A. S., Arslan, Ş., Mutlu, D., Otur, Ç., & Kurt Kızıldoğan, A. (2022). A thiophene derivative, 2-bromo-5-(2-(methylthio)phenyl) thiophene, has effective anticancer potential with other biological properties. *ChemistrySelect*, *7*(15), e202200784. https://doi.org/10.1002/slct.202200784

Zarei, O., Azimian, F., Hamzeh-Mivehroud, M., Shahbazi Mojarrad, J., Hemmati, S., & Dastmalchi, S. (2020). "Design, synthesis, and biological evaluation of novel benzo[b]thiophene-diaryl urea derivatives as potential anticancer agents". *Med. Chem. Res.*, ***29***, 1438–1448. https://doi.org/10.1007/s00044-020-02559-8

Zhang, W., Ma, T., Li, S., Yang, Y., Guo, J., Yu, W., & Kong, L. (2017). "Antagonizing STAT3 activation with benzo[b]thiophene 1,1-dioxide based small molecules". *Eur. J. Med. Chem.*, ***125***, 538–550. https://doi.org/10.1016/j.ejmech.2016.09.068

Zhao, H., Wu, L., Yan, G., Chen, Y., Zhou, M., Wu, Y., & Li, Y. (2021). "Inflammation and tumor progression: signaling pathways and targeted intervention. Signal Transduct ". *Target. Ther.*, ***6***, 263. https://doi.org/10.1038/s41392-021-00658-5